Int. J. Multiphase Flow Vol. 10, No. 5, pp. 623–633, 1984
Printed in the U.S.A.

0301–9322/84 $3.00 + .00
Pergamon/Elsevier

A STUDY OF FLOC BREAKUP AND FORMATION IN FLOWING CONCENTRATED FIBER SUSPENSIONS

EVARISTO J. BONANO†
The Institute of Paper Chemistry, Appleton, WI 54912, U.S.A.

(*Received* 21 *June* 1983; *in revised form* 17 *October* 1983)

Abstract—An experimental study was carried out to examine the effects of fiber concentration and average flow velocity on the breakup of fiber flocs and the subsequent reflocculation process downstream of a converging/diverging flow section used as a turbulence generator. Flocculation measurements were made using fiber optic probes and are presented in terms of floc-size distributions. These were complemented with pressure fluctuation measurements used to indicate the state of fluidization of the suspension.

INTRODUCTION

During the formation of a sheet of paper, good dispersion of the individual fibers is necessary to insure good mechanical properties of the product. However, wood fibers in a suspension undergoing deformation have an inherent tendency to interact with each other and form aggregates (flocs) due to mechanical entanglement (Mason 1948). Thus, prior to dispersing the fibers, the flocs must be effectively disrupted. Because this process is facilitated at lower fiber concentrations, paper is usually formed from dilute suspensions. Papermaking under these conditions requires handling large amounts of water, which in turn, results in excessive size of the equipment.

One approach for reducing the size of papermaking equipment and possibly its operating costs is to form paper from a concentrated suspension, known in the paper industry as "high-consistency forming" (Meyer 1976; Wahren 1979). Several studies have examined the feasibility of such an approach. Currently, high-consistency pilot formers perform two operations: (1) generation of turbulence levels sufficient to break up the fiber flocs and disperse the fibers and (2) formation of a homogeneous fiber network as the turbulence decays (Grundström *et al.* 1973). Their use potentially eliminates the need for the wire section of paper machines used to drain water from the web and consolidate the sheet of paper (Grundström *et al.* 1976). The web leaving these high-consistency formers typically contains the same percentage of fibers by weight as that leaving the wire section in conventional paper machines.

Paper formed from concentrated suspensions tends to have a more felted structure than its counterpart formed from dilute ones. This felted structure has a high porosity which facilitates water removal from the web; also, it is considered the main contributing factor to the poor tensile strength of the paper; compressive strength may actually be acceptable. Fundamental to improving this tensile strength is the ability to align the fibers prior to the formation of the fiber network as the turbulence decays to produce a sheet of paper with a layered structure similar to that obtained from dilute suspensions. Fiber alignment requires breakup of the flocs, followed by maintenance of a floc-free state for the necessary period of time.

Floc breakup and formation are competing effects that are both promoted by turbulence (Wahren 1979). However, studies of turbulent flow of fiber suspensions (e.g. Kerekes & Garner 1982) have demonstrated that even at low concentrations the presence of the fibers attenuates the turbulence. This effect is accentuated with increasing fiber concentration. Furthermore, there is some experimental and theoretical evidence that the mobility of fibers relative to their suspending medium is hindered as concentration

†Present address: Sandia National Laboratories, Albuquerque, NM 87185, U.S.A.

increases (Giebner 1982; Goddard *et al.* 1982). Thus, it seems possible, that while intuitively it is expected that an increase in fiber concentration promotes flocculation, under given sets of conditions the effect may be the opposite. It was the purpose of this study to examine the effects of average flow velocity (the complex rheology of fiber suspension does not allow the proper definition of a viscosity and hence of a Reynolds number) and fiber concentration on the breakup of flocs through a turbulence generator and the reflocculation process in the downstream section for relatively concentrated suspensions. Studies reported in the literature have dealt only with dilute suspensions since conventional turbulence-measuring techniques fail at higher concentrations (Kerekes 1983).

EXPERIMENTAL EQUIPMENT

The experiments were performed in the flow system depicted in figure 1. It consisted of a flow channel of rectangular cross section (0.1524 m × 0.0127 m), a storage tank with a mixer for the fiber suspension, a centrifugal pump, a magnetic flowmeter and a recirculation loop. The fibers were continuously recirculated for the duration of an experiment with an average residence time in the storage tank of about 60 s. Approx. 1.5 m downstream of the inlet to the channel is a converging/diverging section shown in figure 2 (not drawn to scale) used as a turbulence generator. This particular design was chosen because it resembles typical pilot devices used in paper forming from concentrated suspensions. At the constriction (separation = 0.005 m) the average flow velocity was 2.5 times higher than in the upstream section of the channel. The turbulent wake generated at this point caused the breakup of flocs. Also shown in figure 2 are the locations of the fiber optic probes and pressure transducers used to measure the state of floculation of the suspension and pressure fluctuations, respectively. The fiber optic probes covered a distance up to 0.13 m downstream of the trailing edge of the diverging section, and the locations of the pressure transducers extended to 0.15 m.

The y-shaped fiber optic probes (shown in figure 3) used in this study were similar to those previously used for flocculation measurements in fiber suspensions (Appel 1971; Nerelius *et al.* 1972). Each probe consists of two separate bundles of light guides coming together at one end. One was used to carry light from a source to the common end which was mounted flush with the bottom plate of the channel. The light was transmitted into the suspension and the fraction reflected by the passing flocs was carried by the other bundle of light guides to the photodiode which converted the fluctuating light into a fluctuating analog signal.

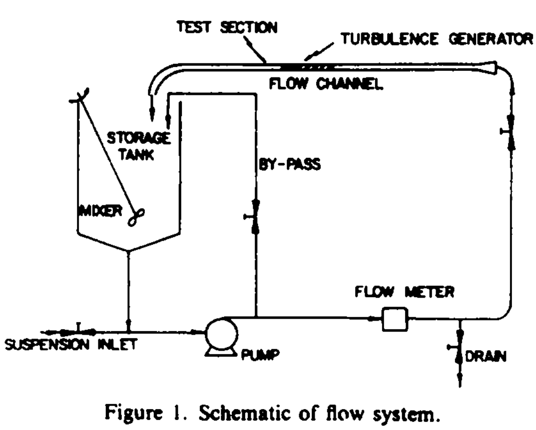

Figure 1. Schematic of flow system.

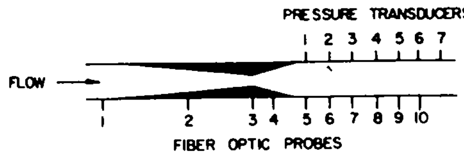

FIBER OPTIC PROBE	PRESSURE TRANSDUCER	DISTANCE FROM TURBULENCE GENERATOR (mm)
5	1	7.94
6	2	31.75
7	3	55.56
8	4	79.37
9	5	103.19
10	6	127.00
	7	150.00

Figure 2. Schematic of converging/diverging section used as turbulence generator and location of fiber optic probes and pressure transducers.

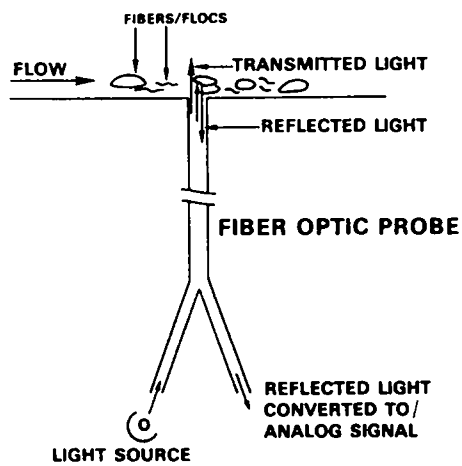

Figure 3. Schematic of fiber optic probe.

The analog signal was sampled using a Tracor Northern 1710 data acquisition unit equipped with a Fast Fourier Transform (FFT) module. The sampling frequency was varied according to the flow velocity; values as high as 100 kHz were used. Power spectral density functions (PSD) were calculated from the sampled signals using the FFT module. The PSD as a function of frequency at a given velocity, is directly related to the size distribution of flocs in the suspension, since the intermittency of the reflected light depended on their size.

The flocculation measurements were complemented with the measurements of the intensity of pressure fluctuations at the wall of the channel using pressure transducers to determine the relative state of fluidization of the suspension. This same technique has been previously used for similar measurements in solid/gas systems (Abed 1982; Tsuji & Morikawa 1982).

RESULTS

The fibers used in this study were softwood bleached kraft pulp fibers with the length distribution shown in figure 4. The majority of the fibers had length in the range of 0.5–2.0 mm. The arithmetic and weighted average fiber lengths were 1.9 and 2.6 mm, respectively. The concentration of fibers in suspension was expressed as percent by weight

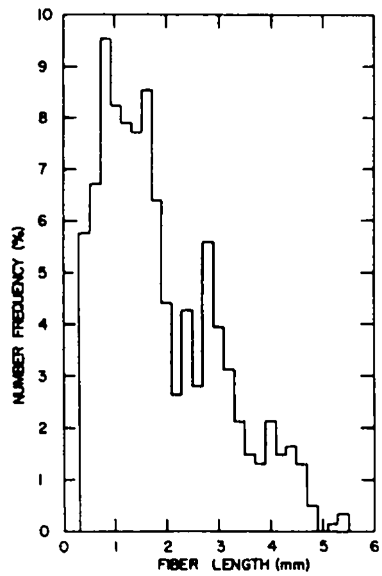

Figure 4. Length distribution of fibers.

of ovendry fibres, i.e.

$$C(\%) = \left[\frac{\text{weight of ovendry fibers}}{\text{weight of ovendry fibers} + \text{weight of water}}\right] \times 100\%.$$

This conventionalism is used throughout the pulp and paper industry, and we have adopted it here. From a hydrodynamics viewpoint, it is the volume concentration of the fibers in suspension that is important. However, because of the hygroscopic nature of cellulose, wood fibers in a wet state absorb water, and the determination of the amount absorbed is rather tedious and difficult. Since we used fibers of only one type, it is reasonable to express their concentration in the manner discussed above.

The amount of light reflected by the fibers in suspension, in principle, should increase linearly with concentration. At high concentrations, complex light scattering effects become a dominant factor, and the relation of reflected light to concentration ceases to be linear. It is essential to determine the concentration at which nonlinear effects set in because it establishes the maximum concentration for which the fiber optic probes are suitable. Figure 5 is a plot of the intensity of reflected light expressed in millivolts as a function of fiber concentration for fiber optic probe 1 at an average velocity of 10.2 m/s. Up to $C = 3\%$, the response with increasing concentration is linear within 4%. Beyond this concentration, nonlinear effects became important. Other probes behave similarly at this and other velocities. We limit the results discussed below to $C = 1\%$ and 2%. These fiber concentrations, although not considered high with respect to other papermaking operations, are nevertheless higher than those from which paper is conventionally formed ($C < 1\%$, typically $\sim 0.5\%$).

The differences in the calibration curves of the different photodiodes and light guides were built into the PSD. To compare the floc size distribution curves at the different locations in the test section, the PSD's were normalized with the r.m.s. value of reflected light for the corresponding probe to obtain a relative power spectral density function (RPSD) given by

$$\text{RPSD} = \text{PSD}/\overline{c'^2}.$$

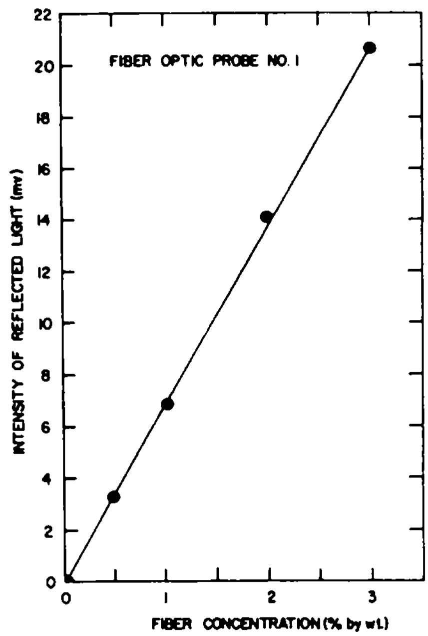

Figure 5. Intensity of reflected light vs fiber concentration for fiber optic probe 1 at $\bar{u} = 10.2$ m/s.

Furthermore, the RPSD's were converted from a frequency to a wavelength domain using the expressions

$$l = \bar{u}/f$$

and

$$\text{RPSD}(l) = (f^2/\bar{u})\,\text{RPSD}\,(f)$$

in order to make the velocity effects more discernible. Thus, RPSD(l) represents the relative occurrence of flocs of different wavelengths l. Data were taken at all probe locations shown in figure 2. However, we present here only the results for probes 1, 5, 7 and 10 because they provide an adequate picture of the change in flocculation across the turbulence generator and the process downstream.

Effect of average flow velocity

Figures 6–8 are plots of RPSD vs l for a suspension with fiber concentration $C = 1\%$ at $\bar{u} = 7.6$, 9.1 and 10.2 m/s, respectively. These velocities are typical of some papermaking operations. The curves are marked 1, 5, 7 and 10 to denote the size distribution at the locations of probes 1, 5, 7 and 10, respectively. At $\bar{u} = 7.6$ m/s, the curves in figure 6 indicate that, as the suspension flowed through the converging/diverging channel, the number of flocs in the approximate range $2.4 < l < 9$ mm experienced a slight net reduction, while those corresponding to $1.5 < l < 2.4$ mm and $l > 10$ mm increased. Downstream of the turbulence generator the fraction of both the larger and smaller flocs decreased, and the size distribution curve became similar to that upstream (curve 1). It is also noticed that the size distribution curves 7 and 10 are not significantly different, an indication that the flocs may have attained a steady-state size distribution between locations 5 and 7.

Increasing the velocity to 9.1 m/s (figure 7) resulted in a net reduction of flocs over a

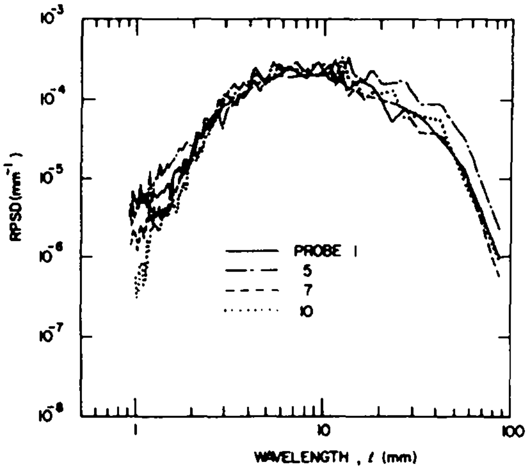

Figure 6. RPSD curves for $C = 1\%$ at $\bar{u} = 7.6$ m/s.

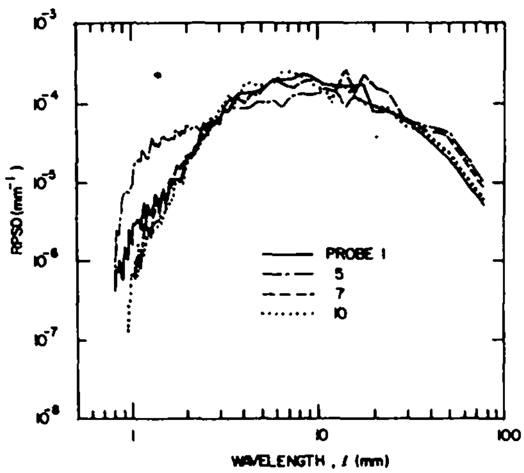

Figure 7. RPSD curves for $C = 1\%$ at $\bar{u} = 9.1$ m/s.

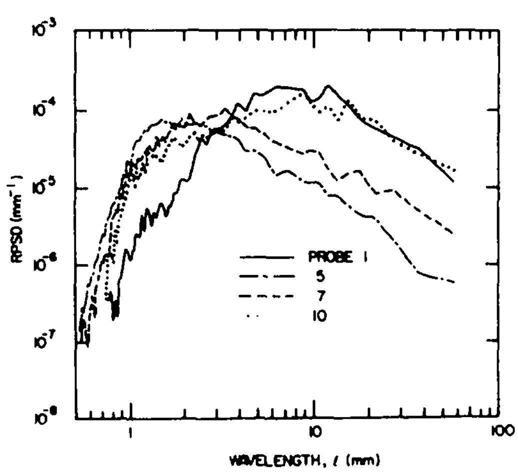

Figure 8. RPSD curves for $C = 1\%$ at $\bar{u} = 10.2$ m/s.

wider size range than at 7.6 m/s, $3 \leqslant l \leqslant 20$ mm. The larger stresses generated within the turbulence generator at the higher velocities were able to disrupt larger flocs more effectively. Still, at this velocity, the numbers of the largest and smallest flocs both increased across the turbulence generator. The increase in the relative fraction of the latter, however, was considerably higher than at 7.6 m/s. Downstream of the turbulence generator, due to the higher velocity, the mobility of the fibers was higher, and the reflocculation process occurred at a faster rate than at 7.6 m/s. In contrast to the previous case, at this velocity the larger flocs did not reach a steady-state size distribution prior to probe 7. The increase in the number of large flocs observed here as the suspension flowed through the converging/diverging section was also observed by Duffy & Norman (1979) for flow through a constriction.

The disruption of flocs at $\bar{u} = 10.2$ m/s (figure 8) was significantly higher compared to that at the lower velocities discussed above. The maximum in the size distribution curve shifted from 5 to 9 mm upstream (curve 1) to close to 1.5 mm immediately downstream (curve 5) of the turbulence generator. The largest flocs were practically all disrupted. Because of the higher velocity, the reflocculation process took place at a much faster rate than before, and the number of large flocs eventually increased and reached a value comparable to that in the upstream distribution (curve 1). Still, a considerable number of small flocs of fibers existed at the location of probe 10. The net depletion occurred for the intermediate size flocs. As the turbulence decayed, the relative fiber motion possibly also decayed, and large flocs in the form of a continuous network were formed.

The amplitude of the pressure fluctuations ($\sqrt{\overline{p'^2}}$) is plotted as a function of position downstream of the turbulence generator in figure 9. At $\bar{u} = 7.6$ and 9.1 m/s as a result of the existence of more of the larger flocs as shown by floc-size distribution curve 5 in figures 6 and 7, the pressure fluctuations were more intense. As the suspension attained a steady-state size distribution which was accompanied by the disappearance of the larger flocs, the intensity of the pressure fluctuations decreased. As the large flocs disappeared downstream of the turbulence generator at $\bar{u} = 7.6$ m/s, the pressure fluctuations decreased and reached a constant value at 80 mm, since the suspension attained a steady-state size distribution. At $\bar{u} = 9.1$ m/s, the pressure fluctuations experienced a sharper decrease due to the disappearance of the larger flocs and the presence of a significant number of the smaller ones. At $\bar{u} = 10.2$ m/s, consistent with the large number of small flocs (possibly fibers) present immediately downstream of the turbulence generator, the intensity of the

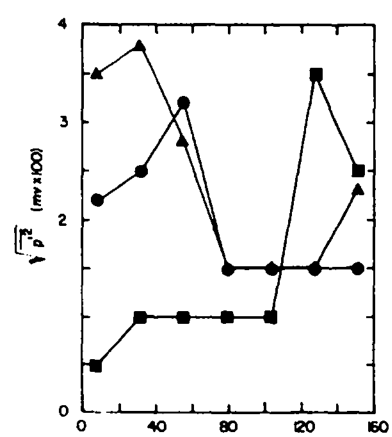

Figure 9. Intensity of pressure fluctuations as function of position downstream of turbulence generator for $C = 1\%$, at $\bar{u} = 7.6$ m/s ●; 9.2 m/s ▲; and 10.1 m/s ■.

pressure fluctuations was low and fairly constant up to a distance of 0.1 m; beyond this position it increases. Size distribution curve 10 (figure 8), which corresponds to a distance of 0.127 m, shows an increase in the relative number of the larger flocs, which causes the increase in the intensity of the pressure fluctuations.

Effect of fiber concentration

The effect of increasing the fiber concentration was examined by comparing floc-size distribution curves at 9.1 and 10.2 m/s for $C = 2\%$ with the respective curves at $C = 1\%$. At 7.6 m/s the size distributions obtained at this higher concentration were qualitatively the same as those for the 1% suspension, and therefore we need not discuss them here. Figures 10 and 11 show the size distribution curves at 9.1 and 10.2 m/s, respectively, for $C = 2\%$. The corresponding intensities of the pressure fluctuations as functions of position downstream of the turbulence generator are plotted in figure 12.

Comparison of the size distribution curves in figure 10 with those in figure 7 indicates a somewhat unexpected effect of the higher fiber concentration in the disruption of flocs. For $C = 1\%$, at $\bar{u} = 9.1$ m/s, the number of the larger flocs increased as the suspension travelled across the turbulence generator (see figure 7). On the other hand, at $C = 2\%$, these practically disappeared completely. This could have resulted because the flocs of increasing size associated with the higher fiber concentration may be easier to disrupt than smaller ones. The effect of the higher fiber concentration on the reflocculation process is also evident from the curves in figure 10. We notice that far downstream of the turbulence generator (probe 10) the fraction of the largest flocs increased considerably at the expense of the smallest ones, but the fraction of the latter remained considerably higher compared with the upstream size distribution (probe 1). At 10.1 m/s (figure 11), the breakup of flocs was qualitatively the same as for $C = 1\%$ at this same velocity, the difference being on the fraction of single fibers still apparent in curve 10 compared with curve 5. For $C = 2\%$, a large fraction of the latter seems to still be present compared with the same curve for $C = 1\%$.

The intensity of the pressure fluctuations for $C = 2\%$ are presented in figure 12. At $\bar{u} = 9.1$ m/s, the maximum in the pressure fluctuations occurs at the location of probe 7 ($\sim$55 mm) where curve 7 in figure 10 shows a significant increase in the fraction of the large flocs. The decrease downstream of probe 7 was likely due to the formation of uniform large flocs as indicated by curve 10 in figure 10. Tsuji & Morikawa (1982) observed a similar behavior in the intensity of pressure fluctuations in systems of small solid particles

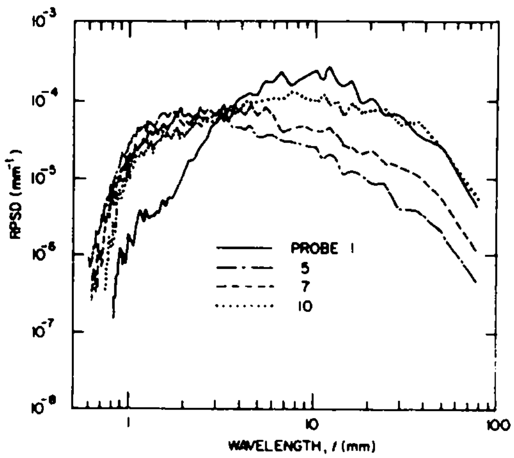

Figure 10. RPSD curves for $C = 2\%$ at $\bar{u} = 9.1$ m/s.

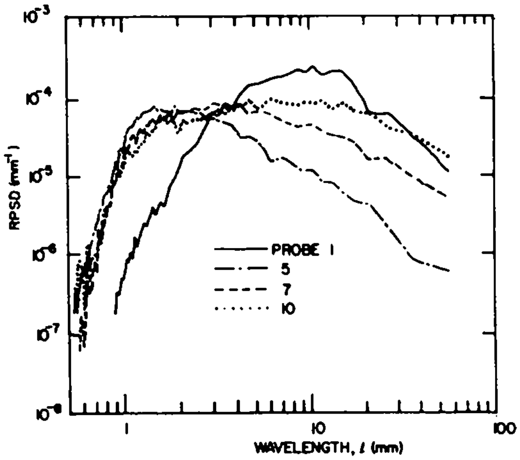

Figure 11. RPSD curves for $C = 2\%$ at $\bar{u} = 10.2$ m/s.

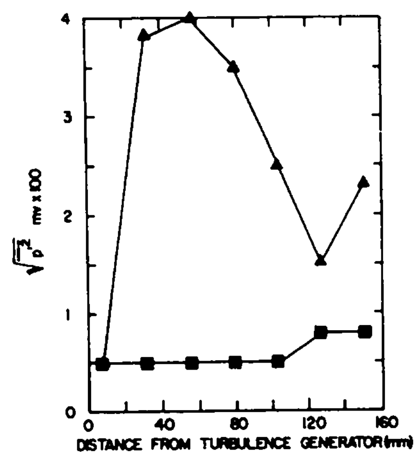

Figure 12. Intensity of pressure fluctuations as function of position downstream of turbulence generator for $C = 2\%$, at $\bar{u} = 9.1$ m/s ▲; and 10.1 m/s ■.

being conveyed in an air stream. They show that as the average velocity decreased, the particles clustered to form aggregates and consequently, the intensity of the pressure fluctuations increased. A further decrease in velocity resulted in the particles forming a uniform bed which was accompanied by less intense pressure fluctuations. At $\bar{u} = 10.1$ m/s, the pressure fluctuations we measured remained uniform and low up to the last 25 mm of the test section, at which they slightly increased. At this velocity, still at the location of probe 10 (figure 11), a significant number of small flocs or fibers exist, whereas that of larger flocs did not reach the levels existing at probe 1.

The effect of increasing fiber concentration could not be completely elucidated from the size distribution curves presented here. At $\bar{u} = 9.1$ m/s, for $C = 2\%$ large, possibly uniform flocs seem to form faster compared with the 1% suspension judging from the pressure fluctuations. On the other hand, at $\bar{u} = 10.2$ m/s, at the higher fiber concentration, the reflocculation was possibly retarded as indicated by comparing curve 10 in figures 8 and 11. Our continuing experimental work is attempting to answer the questions that arose from the present study.

CONCLUSIONS

An experimental study has been conducted in which the effects of fiber concentration and velocity on the size distribution of fiber flocs across a turbulence generator and downstream of the latter have been examined. The flocculation measurements were complemented with measurements of the intensity of pressure fluctuations, which provided an indication of the state of fluidization of the suspension. Due to the upper limit on concentration set by the fiber optic probes the data was limited to two concentrations, nevertheless, some trends were clearly observed and are summarized as follows:

(1) At low velocities, the generated turbulence levels are not sufficiently high to disrupt large flocs. In turn, the interaction of smaller flocs or fibers is increased resulting in the formation of larger ones.

(2) After their size distribution is disturbed by turbulence generation, the flocs in a fiber suspension, given a sufficiently long distance, will attain a steady-state size distribution. The distance required depends on average flow velocity and fiber concentration. Increasing the velocity results in increasing the length required for the suspension to attain such steady-state, floc-size distribution.

(3) The larger flocs at higher fiber concentrations, at a given velocity, are disrupted more effectively. The effect of increasing fiber concentration on the reflocculation process is to promote the reflocculation process under certain conditions while impeding it under others.

(4) Measurements of the intensity of the pressure fluctuations are consistent with the flocculation measurements and establish the state of fluidization of the suspension. It may prove an effective technique in extending the experiments to fiber concentrations beyond the useful range of the fiber optic probes.

Acknowledgements—This work was carried out under Project 3479 at The Institute of Paper Chemistry. The author is indebted to D. P. Swoboda without whom this work could not have been performed. M. Gabrielski and R. Tyler also deserve recognition for maintaining the equipment in good working condition. The many suggestions of Dr. D. Wahren are also much appreciated.

REFERENCES

ABED, R. 1982 The characterization of fluidized nonuniformity in large fluidized beds. Paper 80a, AIChE 1982 Annual Meeting, Los Angeles, CA, 14–19 Nov. 1982.

APPEL, D. W. 1971 Measurements of flocculation in flows of fiber suspensions through nozzles, *Proc. 26th TAPPI Engineering Conf.*, pp. 345–360.

DUFFY, G. G. & NORMAN, B. G. 1979 Fiber flocculation in conical contractions simulating the paper machine flowbox slice. *Proc. Int. Symp. on Paper Machine Headboxes*, pp. 43–53. McGill Univ., Montreal, Quebec, Canada, 3–5 June 1979.

GIEBNER, H. R. 1982 The response of higher consistency fiber suspension to shear forces. *M. S. Report*. The Institute of Paper Chemistry, Appleton, WI.

GODDARD, J. D., HUANG, Y.-H. & HUANG, L.-C. 1982 Rational prediction of composite properties based on asymptotic micromechanics. *Proc. 9th U.S. Congress in Applied Mechanics, Am. Soc. Mech. Engng* 197–211.

GRUNDSTRÖM, K.-J., MEINANDER, P. O., NORMAN, B., REINER, L. & WARIS, T. 1976 A high-consistency former. *Tappi* **59**, 58–61.

GRUNDSTRÖM, K.-J., NORMAN, B. & WAHREN, D. 1973 High consistency forming of paper. *Tappi* **56**, 81–84.

KEREKES, R. J. 1983 Pulp flocculation in decaying turbulence: a literature review. *J. Pulp Paper Sci.* (*Trans. CPPA*), TR86–91.

KEREKES, R. J. & GARNER, R. G. 1982 Measurement of turbulence in pulp suspensions by laser anemometry. *Trans. CPPA* **83**, TR53–60.

MEYER, E. G. 1976 Feasibility of high consistency forming. *Tappi* **59**, 56–57.

MASON, S. G. 1948 The flocculation of cellulose fiber suspensions. *Pulp & Paper Mag. Can.* **49**, 99–104.

NERELIUS, L., NORMAN, B. & WAHREN, D. 1972 Measurement of flocculation characteristics by light reflection. *Tappi* **55**, 574–580.

TSUJI, Y. & MORIKAWA, Y. 1982 Flow pattern and pressure fluctuation in air–solid two-phase flow in a pipe at low air velocities. *Int. J. Multiphase Flow* **8**, 329–341.

WAHREN, D. 1979 Fiber network structures in papermaking operations. *Proc. Conf. Paper Science and Technology—The Cutting Edge* pp. 112–129. The Institute of Paper Chemistry, Appleton, WI, 8–10 May 1979.